Hierarchic Supramolecular Interactions within Assemblies in Solution and in the Crystal of 2,3,6,7-Tetrasubstituted 5,5′-(Anthracene-9,10-diyl)bis[pyrimidin-2-amines][1])

by **Teodor Silviu Balaban**[a])[2]), **Andreas Eichhöfer**[a])[3]), **Michael J. Krische**[b])[4]), and **Jean-Marie Lehn**[a])[c])[5])

[a]) Forschungszentrum Karlsruhe, Institute for Nanotechnology, Postfach 3640, D-76021 Karlsruhe
[b]) University of Texas at Austin, Department of Chemistry and Biochemistry, Welch Hall, Austin, TX 78712, USA
[c]) ISIS, Université Louis Pasteur, 8 Allée Gaspard Monge, BP 70028, F-67083 Strasbourg

The title compounds **6** and **7** were synthesized in good yield (*Schemes 1* and *2*), and their mode of assembly was studied both in solution, for the tetrakis(decyloxy) derivative **6**, and in the crystal, for the tetramethoxy analogue **7**. The pyrimidin-2-amine moieties of **6** and **7** can engage in three different supramolecular interactions: *i*) metal ligation *via* one of the pyrimidine N-atoms, *ii*) cooperative double H-bonding *via* the NH_2 group, and *iii*) π–π-stacking interactions. In solution, coordination of the central Zn-atom within the soluble porphyrinatozinc complex **19** leads to significant changes in the NMR and absorption spectra of **6**. In the absence of metal ligation, the next strongest interaction is H-bonding which can operate in nonpolar or moderately polar solvents. In these cases, however, no stacking interaction or inclusion compounds could be put into evidence in the case of **6** by absorption, fluorescence, or NMR spectroscopies. The π-stacking interactions were only observed in the crystal of **7** in conjunction with double H-bonding. Slightly disordered DMSO molecules are also H-bonded to the NH_2 groups of **7**, perturbing the expected packing. The present study illustrates some of the challenges inherent to directing hierarchical assembly processes in the solid state.

Introduction. – Pyrimidin-2-amine (2PA) is a versatile recognition group which has been used to decorate tectons with the scope of programed self-assembly [1–4]. It can simultaneously engage in three different supramolecular interactions: *i*) metal ligation, *ii*) cooperative double H-bonding, and *iii*) π-stacking. Porphyrinatozinc complex **1** which has a single 2PA recognition group assembles into tetramers both in solution and in the crystal (*Fig. 1*) [4]. Tetramer formation is directed by the *meta*-position of the two endocyclic N-atoms of the pyrimidine moiety, one of which coordinates the central Zn-atom within the tetrapyrrole core of an adjacent porphyrinato ligand. Within the tetramer's interior, although energetically less stabilizing, two 2PA groups prefer to π-stack instead of engaging in double H-bonding. In the crystal, the two other

[1]) For previous papers about pyrimidin-2-amine (=2-aminopyrimidine) as a recognition group, see [1–4].
[2]) Materials and methods or general questions: fax: +49 724 782 8298; e-mail: silviu.balaban@int.fzk.de.
[3]) Crystallographic issues: fax: +49 724 782 6368; e-mail: eichhoefer@int.fzk.de.
[4]) Pyrimidin-2-amine directed self-assembly: fax: +1 512 471 8696; e-mail: mkrische@mail.utexas.edu.
[5]) Other issues: fax: +33 390 24 11 17; e-mail: lehn@chimie.u-strasbg.fr.

2PA groups, which point to the tetramer's exterior, lead to an infinite strand of tetramers stitched together by double H-bonding as shown in *Fig. 1*. The generality of tetramer formation was more recently established with the related porphyrinatozinc complexes **2** [5] and **3** [6] which both have a *meso*-pyridin-3-yl group, *i.e.*, a *meta*-positioned N-atom. When two 2PA groups are bound to the same porphyrinatozinc as in **4**, oligomers are preferentially formed in solution instead of tetramers [4].

From the earlier work involving 2PA-directed self-assembly [1–3], it is known that, in the absence of metal ligation, double H-bonding occurs in several crystal structures in conjunction with extensive π-stacking interactions. These were used to from clathrates with various aromatic guests or solvent molecules, as indicated schematically in *Fig. 2* by the gray rectangles in the case of the 2PA 5,5′-(anthracene-9,10-diyl)bis[pyrimidin-2-amine] (**5**) [3].

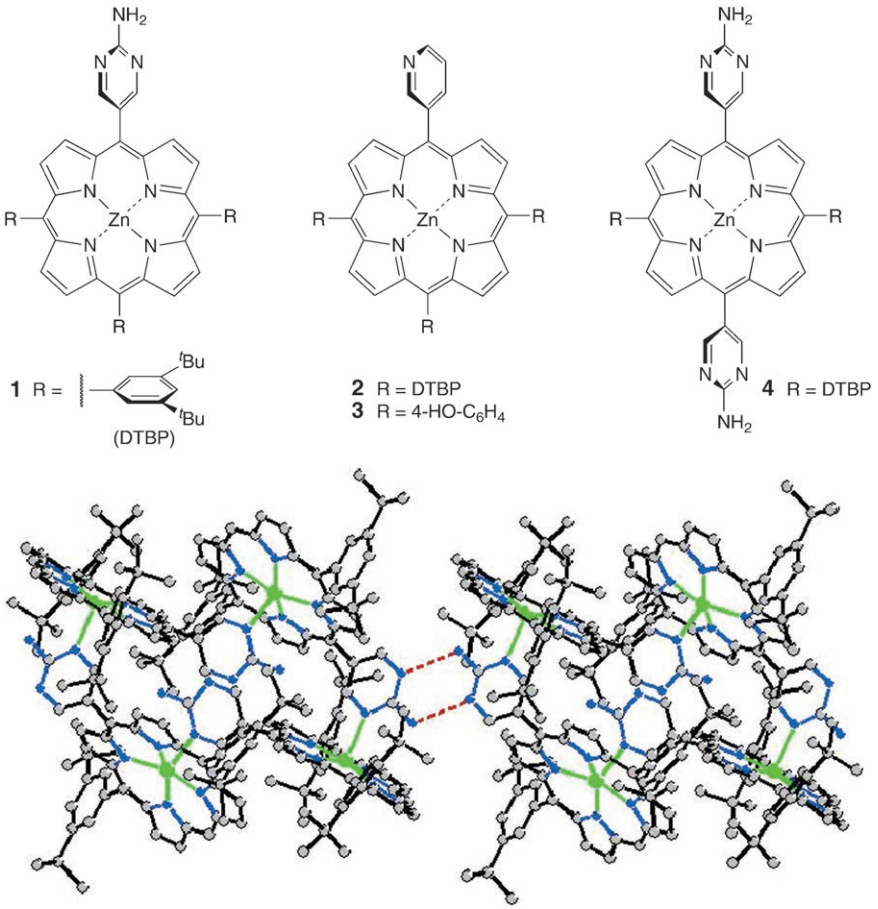

Fig. 1. *Porphyrinatozinc Complexes* **1**–**4** *and doubly H-bonded tetramers of* ***1*** *in the crystal [4]*. DTBP stands for 3,5-di(*tert*-butyl)phenyl which is an excellent solubilizing group introduced to porphyrin chemistry by *Crossley* and *Burn* [7].

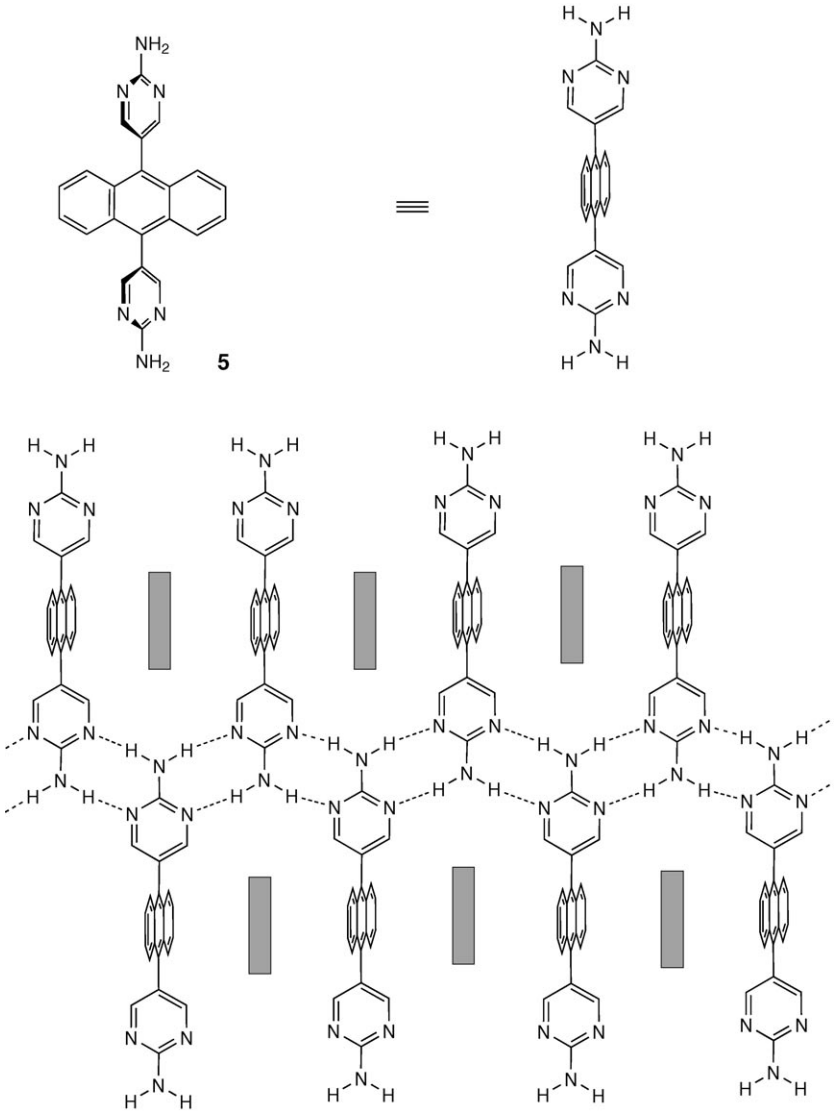

Fig. 2. *Planar tape-like double H-bonding of 5,5′-(anthracen-9,10-diyl)bis[pyrimidin-2-amine]* (**5**) *used to assemble* ca. *7.0-Å voids which in the crystal can bind various aromatic guests such as phenazine* [3]

Because the 2PA-directed self-assembly of the porphyrinatozincs **1** and **4** worked well also in solvents of medium polarity such as $CHCl_3$, we wanted to learn whether, in the absence of metal ligation, similar assemblies as that depicted in *Fig. 2* are formed, not only in the crystal but also in solution, from more soluble (anthracenediyl)bis[pyrimidin-2-amine] derivatives than **5**. Thus, we report here the syntheses of the 5,5′-(anthracene-9,10-diyl)bis[pyrimidin-2-amines] **6** and **7** which are 2,3,5,6-tetrakis(decyloxy)- and 2,3,5,6-tetramethoxy-substituted, respectively, and studies of their self-

assembly which allow us now to draw a hierarchy in 2PA-mediated supramolecular interactions.

Results and Discussion. – *Syntheses.* The synthetic sequence for the preparation of the soluble long-chain derivative **6** is presented in *Scheme 1*. The condensation of veratrol (=1,2-dimethoxybenzene; **8**) with acetaldehyde mediated by H_2SO_4 was performed as described earlier [8], while the oxidation of the Me groups in **9** with $Na_2Cr_2O_7$ in AcOH to the 2,3,6,7-tetramethoxy-9,10-anthraquinone (**10**) and the subsequent hydrolysis of the MeO groups were slightly improved as compared to the methods described by *Boldt* [9] (*Scheme 1*). We consistently obtained **11** in different runs with more than 70% yield over two steps. The alkylation of all four OH groups in **11** with 1-bromodecane was unproblematic, while the reduction of the anthraquinone **12** proved to be more efficient if the intermediate anthracenone **13** was isolated, rather than to attempt a direct reduction to the anthracene **14**.

Scheme 1. *Synthesis of* **6**

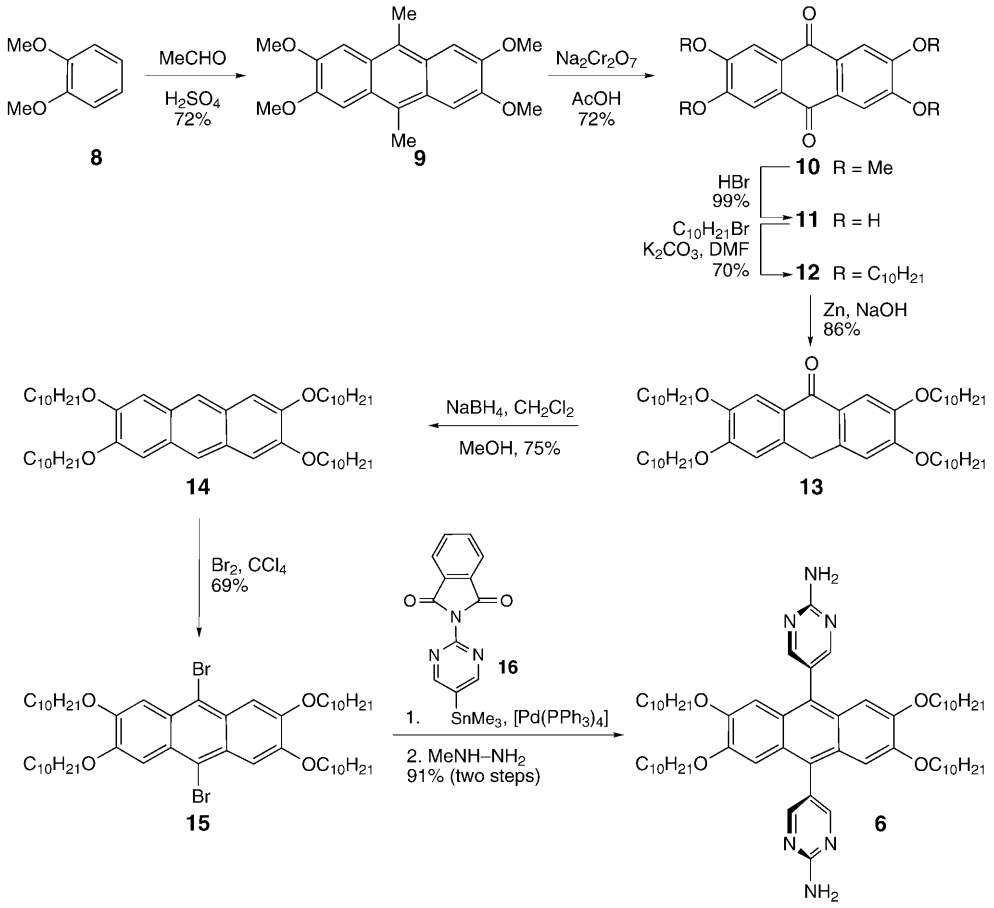

The four long alkoxy whiskers at the anthracene skeleton impart special solubility properties to compound **14**. We especially chose decyl chains because two long-chain decyloxy substituents at C(2) and C(3) of an anthracene skeleton are known to form excellent and fluorescent gelators for organic solvents such as MeOH in minute quantities (<10 μM) [10]. With two hexyloxy chains, the 2,3-disubstituted anthracene could be crystallized with a unit cell composed of 18 monomers which apparently associate into triads which pack into a head-to-tail fashion [11]. Recently, due to its good solubility, compound **14** was used as a guest taking advantage of its π-stacking ability for nanomechanical molecular tweezers which can be conformationally switched by metal coordination [12]. A binding constant of 1020 ± 60 M^{-1} could be measured between **14** and an acridine tweezer in $CDCl_3$ containing 8% CD_3OD. This value allows an estimation of the π–π interactions of a donor-substituted anthracene in the absence of H-bonding (*vide infra*, discussion and conclusions).

Dibromination of **14** and a double *Stille* condensation with the protected stannyl derivative **16** [3] followed by a final deprotection with methylhydrazine completed the reaction sequence. Over nine steps, starting from commercial veratrol (**8**), the global yield of the desired product **6** with long chains was thus 15%. Gratifying was that the optimized Pd-catalyzed double *Stille* coupling and phthalimide deprotection [3] functioned so well that the two final steps of the sequence were very high-yielding (91% over two steps) and thus accounted for a pronounced atom and catalyst economy [13].

In the somewhat shorter synthesis of the less soluble tetramethoxy derivative **7** (*Scheme 2*) we found that the alkaline zinc reduction of the anthraquinone **10** proceeded as described [14] giving directly the anthracene **17** so that the isolation of the intermediate anthracenone could be avoided. Again we ascribe this striking different reaction progress to the wettability difference imparted by the MeO substituents in **17** in comparison to the decyloxy substituents in **14**. However, in this case, the double *Stille* coupling of **18** could not be driven to completion due to the low solubility so that a rather tedious and low-yielding chromatographic purification of **7** had to be performed to obtain single crystals (see *Exper. Part*).

Self-Assembly Studies in Solution. With compound **6** in hand, which has a good solubility in solvents such as CH_2Cl_2, $CHCl_3$, toluene, or even warm benzene so that ^{13}C-NMR spectra can be recorded within a few hours, we attempted to study the pyrimidin-2-amine induced self-assembly in solution. Neither absorption combined with stationary fluorescence nor NMR spectra gave any indication that the anthracene π-systems are somehow coming into close interactions. No concentration-dependent shifts could be detected in a variety of solvents. Also no shifts were observed upon addition of various guest molecules such as phenazine or 2,3,6,7-tetramethylphenazine [15]. Fluorescence-quenching experiments in $CHCl_3$ showed that upon addition of phenazine, the anthracene fluorescence was quenched similarly in **6** and in **14** (*Fig. 3*), again indicating that preorganization induced by the pyrimidin-2-amine moieties of **6**, does not occur in solution. No attempts were made to see if nonlinear *Stern–Volmer* behavior is encountered.

To exclude that adventitious H_2O could inhibit the H-bonding of the pyrimidin-2-amines, all solvents were thoroughly dried as described in the *Exper. Part*. In (D_6)benzene at 55°, no chemical-shift changes could be observed in the ^{1}H-NMR spec-

Scheme 2. *Synthesis of* **7**[a])

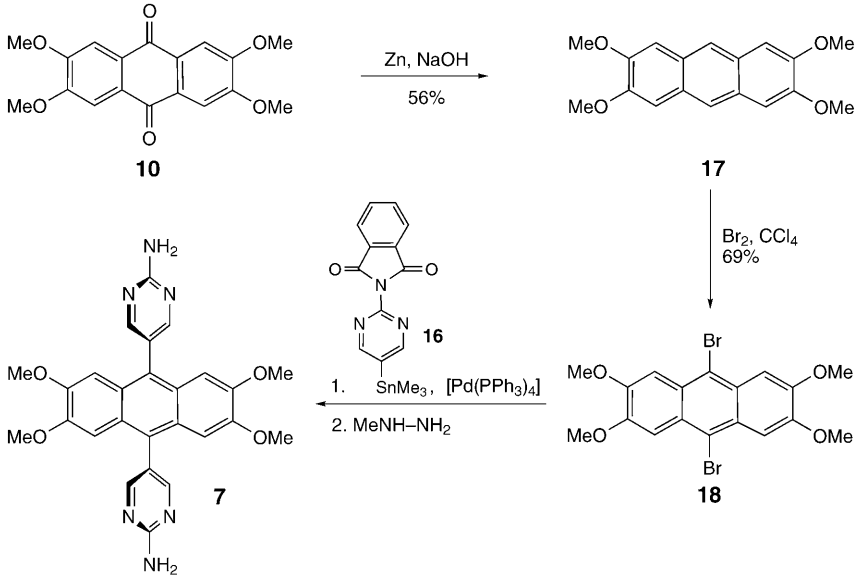

[a]) The yield of the last two reactions in the sequence is not given due to incomplete conversion of the starting material and difficult chromatographic separation. A pure sample of **7** could be isolated in *ca.* 10% yield, although according to TLC and ^{1}H-NMR an analytical yield of >50% could be determined.

tra upon addition of phenazine. However, small shifts for the protons of **6** were observed upon titrating with CD_3OD in the NMR tube, which efficiently disrupts H-bonds. To exclude that these shifts are due to a perturbation of the putative H-bonding network, an additional control experiment was carried out by titrating a solution of pure **6** dissolved in dry $CDCl_3$ with CD_3OD. As seen from *Fig. 4*, the effects are quite small, and we ascribe them to the change in solvent polarity and not to a disruption of the H-bonding network. Note that upon CD_3OD addition, the NH_2 protons become deshielded while the anthracene and pyrimidine protons (data not shown) are slightly shielded.

The above data show that the long chains in **6**, probably due not only to their bulk but also to their hydrophobic nature, hinder formation of an extended H-bonding network in solution which would bring about π-stacking interactions, and of course no association constant could be determined. Furthermore, in the absence of this preorganization, no inclusion complexes are formed upon addition of aromatics with extended π-systems.

Complexation Studies with Porphyrins and Charge-Transfer Acceptors. The ability of the 2PA groups in **6** to coordinate the central Zn-atom within porphyrinato complexes was probed by absorption and NMR spectroscopies in the presence of the very soluble model porphyrinatozinc **19**. We have shown earlier that **19**, in contrast to the isomeric porphyrinatozinc **20**, shows only small variations in chemical shifts over a wide concentration and temperature range [16]. This is because the 1,4-phenyl-

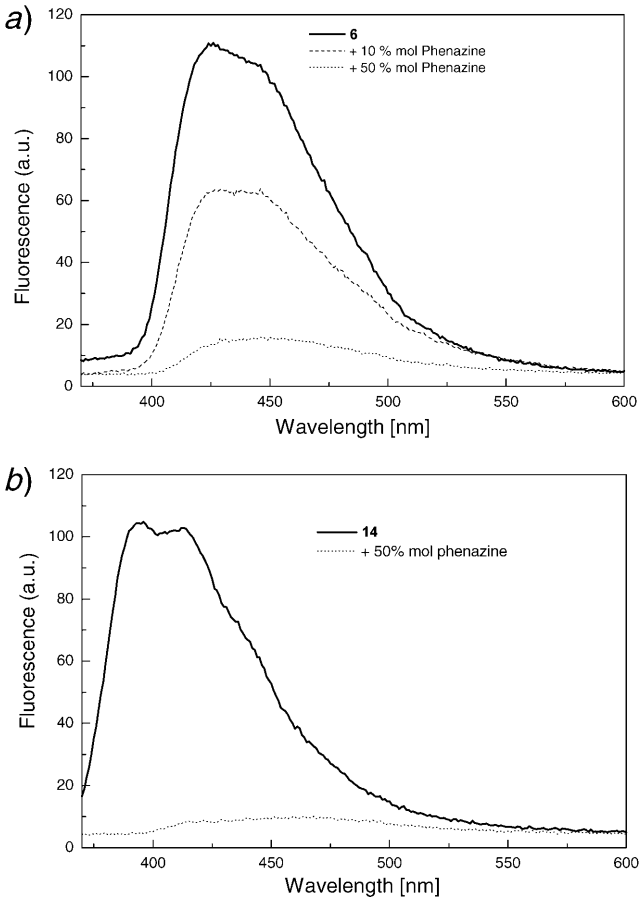

Fig. 3. *Stationary fluorescence quenching experiments with phenazine added to solutions in dry $CHCl_3$ of* a) **6** *and* b) **14**. Pathlength 1 cm.

ene moieties in position 5 and 15, which in homologous crystal structures have a dihedral angle to the porphyrin plane of 65°, allow only a marginal π-stacking interaction [16].

Fig. 5 and *6* present the changes in the NMR spectra of **6** in dry $CDCl_3$, recorded at 25° upon addition of the porphyrin **19**. Significant shieldings of the pyrimidine (H–C(4) and H–C(6)) and α-anthracene signals were observed upon titration with porphyrin **19**. In contrast, the ethereal CH_2O (αCH_2) groups of the decyloxy chains show only a minor upfield shift while the porphyrin protons remain constant.

As seen from *Fig. 5*, beside the upfield shift, the pyrimidine protons experience considerable broadening and eventually become split at 25° and at a 1:1 stoichiometry between **6** and **19** (upper most trace in *Fig. 5,a* and inset). Upon heating to 55°, this signal shifts back downfield and sharpens (*Fig. 5,b*). These changes are perfectly reversible upon cooling. This spectral behavior can only be accounted for either by the formation of two different complexes which are in equilibrium and by the slow exchange limit

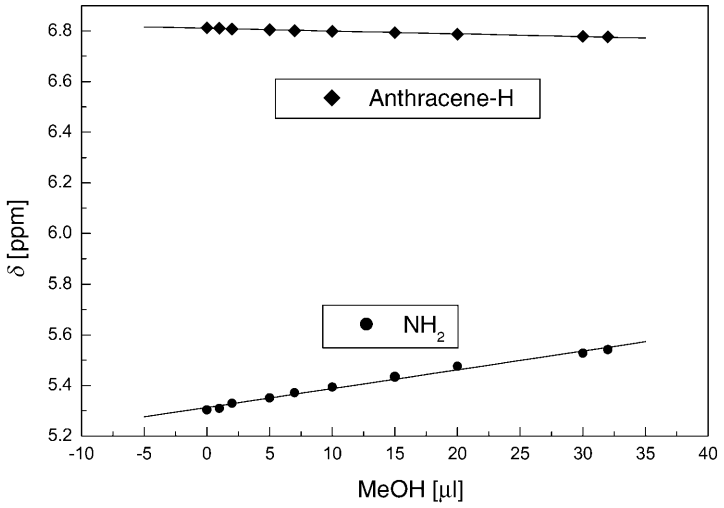

Fig. 4. *Titration of a solution of* **6** *in dry* $CDCl_3$ *at* $40\pm0.5°$ *with* CD_3OD.

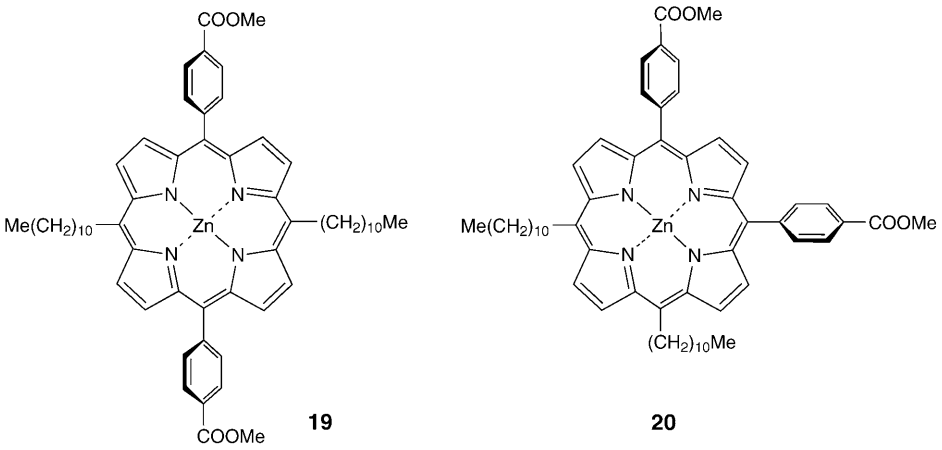

at room temperature on the NMR time scale, or by the magnetic nonequivalence of H–C(4) and H–C(6) of the pyrimidine moiety upon 1:1 complexation of the N(1)-atom. From the crystal structure of **1**, we exclude that complex formation occurs *via* the NH_2 group. With excess **19**, evidently a 1:2 complexation will be favored. Both '*syn*' and '*anti*' conformations are possible in such a $\mathbf{6}\cdot\mathbf{19}_2$ species. While rotation about the (1,4-phenylene)-prophyrin linkage of **19** should be unhindered, at room temperature, the pyrimidine groups of **6** rotate slowly because of the neighboring anthracene H-atoms. The two rotamers, which have different chemical shifts, may equilibrate on the NMR time scale upon heating. Evidently this is not true for absorption or fluorescence where different excitonic interactions are encountered between the opposing prophyrin rings in the two rotamers. *Nakanishi*, *Berova*, and coworkers have systematically studied such interactions in bis-porphyrins covalently linked to chiral skeletons

using circular dichroism [17][18]. Very recently, *Hunter*, *Ballesteros*, and coworkers have studied the complexation behavior of a (tetraarylporphyrinato)zinc with the ditopic N-ligand DABCO (1,4-diazabicyclo[2.2.2]octane) [19]. We expect a very similar and rather complicated spectral behavior in our case. A line-shape analysis which, in principle, could give more information on the multiple equilibria involved was beyond the scope of our present communication. Also the absorption spectra at 1:1 stoichiometry between **6** and **19** show complicated line shapes, indicating the presences of multiple species (data not shown).

Fig. 7 shows probable calculated molecular models of the complex $\mathbf{7}\cdot\mathbf{19}_2$. More complicated architectures, which we cannot exclude, are also envisageable, and we are pursuing crystallization trials both at 1:1 stoichiometries of **7** and **19** and with excess porphyrin **20**. However, due to the presence of multiple long chains, chances to obtain measurable X-ray diffraction patterns are quite small.

With ethenetetracarbonitrile (TCNE), compound **6** formed an interesting charge-transfer (CT) complex of blue color but it could not be isolated in pure form and characterized. While anthracene derivative **6** melts at 248° (and decomposes over 350°), the blue complex did not melt or change its appearance up to 400°. Unchanged **6** which was pale tan-yellow could be recovered in good yields from the complex by washing with acetone. Attempts to obtain mass spectra with a variety of ionization techniques and matrices failed to evidence parent peaks with a molecular mass higher than that of **6**. Elemental analysis for H and N gave results which indicated that probably one molecule of TCNE is present in the complex, although the C-content was consistently lower than the required value. Anthracenes substituted at C(9) are known to form CT complexes with TCNE [21–23]. In the case of the 9,10-[2.2]-*para*-anthracenophane, while in CH_2Cl_2 solution a λ_{max} value of 865 nm was reported for the CT band [23], in the crystal which is of green color, the TCNE molecules lie in an unparallel orientation to the anthracene planes, at an angle of 144° [21], bridging anthracenophanes along the stacking axis. This is quite untypical for other arene·TCNE complexes where the overlap between the HOMO of the arene and the LUMO of TCNE is maximized in a parallel orientation. Apparently, no other crystal structure of an anthracene derivative and TCNE is known. We note in the case of **6**·TCNE that, due to the four alkoxy substituents, the stability of the complex should be increased, and a bathochromic shift of the CT band was observed in comparison to all other known examples.

Co-crystallization experiments of **6** with phenazine from various solvents led in several cases to the isolation of large yellow crystals which, however, proved to be pure phenazine. Thus, no clathrates which could resemble the sponging ability of **5** were formed. Furthermore, several attempts to grow single crystals suitable for X-ray diffraction from pure **6** – over half a decade – invariably failed although several methods, solvent mixtures, and temperature protocols were employed. It is interesting to note that also the parent compound **5** when co-crystallized with anthraquinone instead of phenazine, grows large needles (1–2 cm long) from a DMSO solution but which proved to be only anthraquinone and not a clathrate.

Self-Assembly in the Crystal. Evidence that 2PA-mediated assembly does operate in homologous constructs came from the less soluble compound **7**. We could grow single crystals of **7** suitable for X-ray diffraction by slow evaporation from DMSO. Of course, as the previously synthesized 5,5′-(anthracene-9,10-diyl)bis[pyrimidin-2-amine] (**5**)

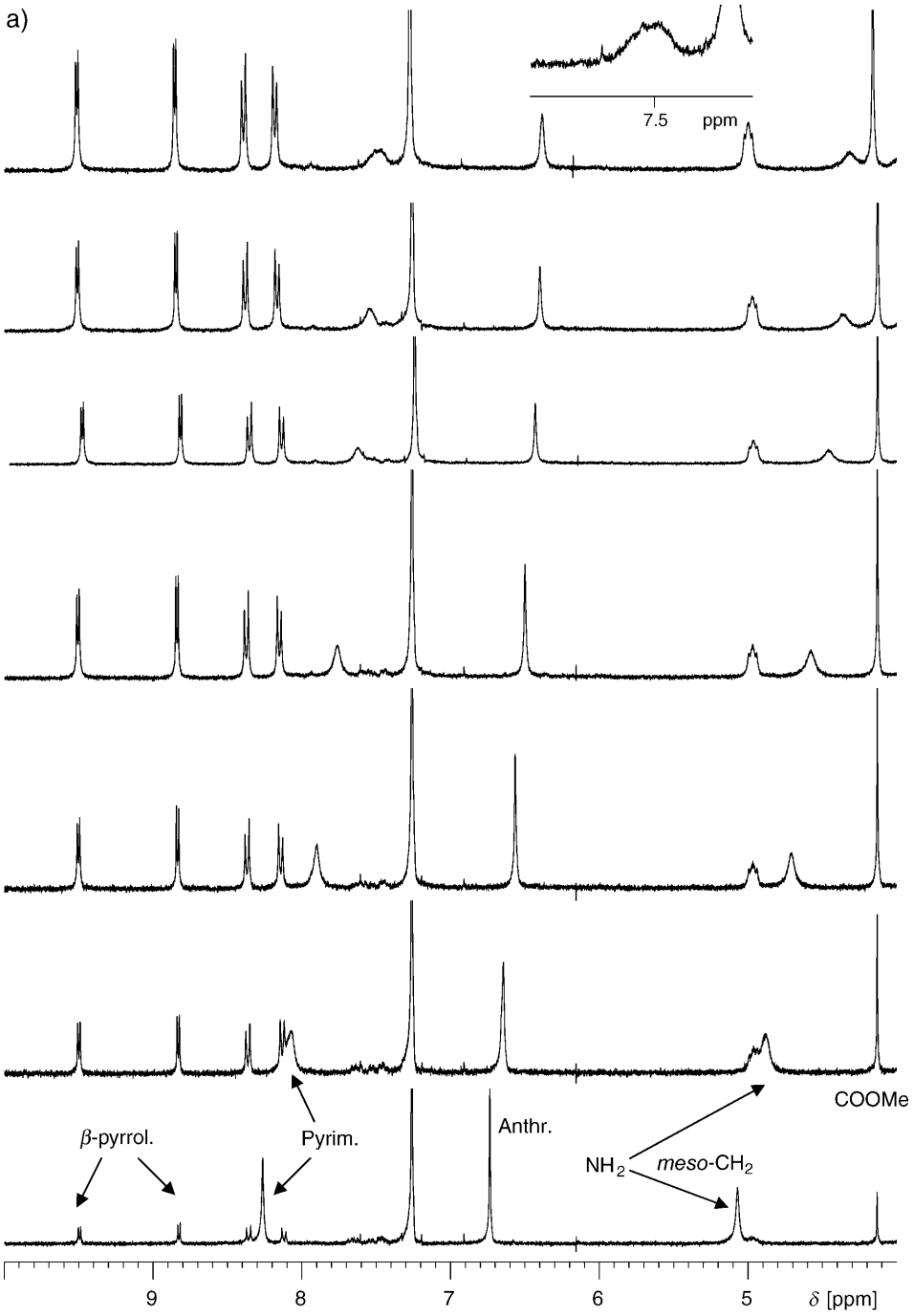

Fig. 5. a) *Low-field region of the* ^{1}*H-NMR spectra* (300 MHz, $CDCl_3$, 25°) *of* **6** *upon addition of porphyrin* **19**. b) *Temperature dependence of the low-field* ^{1}*H-NMR region* (300 MHz, $CDCl_3$) *at a 1:1 stoichiometry between* **6** *and* **19**. Note that the pyrimidine-proton signals, which show a broad and partially complicated splitting at 25°, sharpen and shift to lower field at 35°, but there is hardly any change from 45 to 55°.

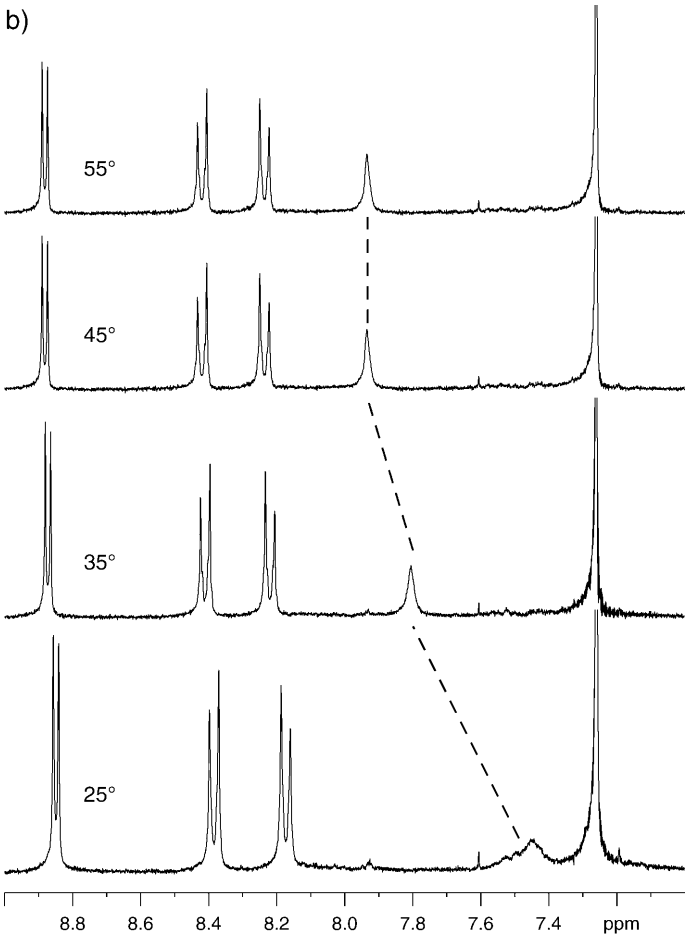

Fig. 5 (cont.)

[1] [2], **7** is completely insoluble in less polar solvents. *Fig. 8* shows the crystal structure of a monomer of **7** which binds two adventitious DMSO molecules to both 2-amino groups which are in an '*anti*'-conformation. The length of the O···H bond is 2.161 Å while the O···H–N angle is 168.6° with an O–N distance of 3.009 Å which document quite tight H-bonding of the solvent.

The programmed double H-bonding self-assembly known to function in the previously described pyrimidin-2-amine crystal structures [1–3] is perturbed in the case of **7** due to the DMSO inclusion which blocks one of the NH H-bonding donor sites. Thus only the other NH can bind to a neighboring N(1) atom of the pyrimidine moiety, forming an extended H-bonding network in one direction which is depicted in *Fig. 9*. In the perpendicular direction, π-stacking assembles the anthracenes in an off-setted geometry as displayed in *Fig. 10*.

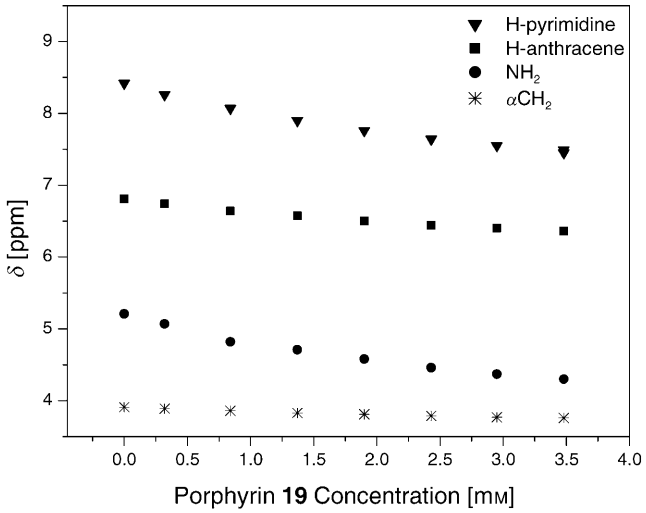

Fig. 6. *Dependency of the* ^{1}*H-NMR chemical shifts* (300 MHz, 25°) *of* **6** *in dry* $CDCl_3$ *on the concentration of added porphyrin* **19**. The initial concentration of **6** was 3.0 mM. Initially 30 µl and then 50 µl aliquots of a 6.3 mM solution of **19** were incrementally added to the NMR tube. Note that the *y*-axis is fourfold expanded in comparison to *Fig. 4*.

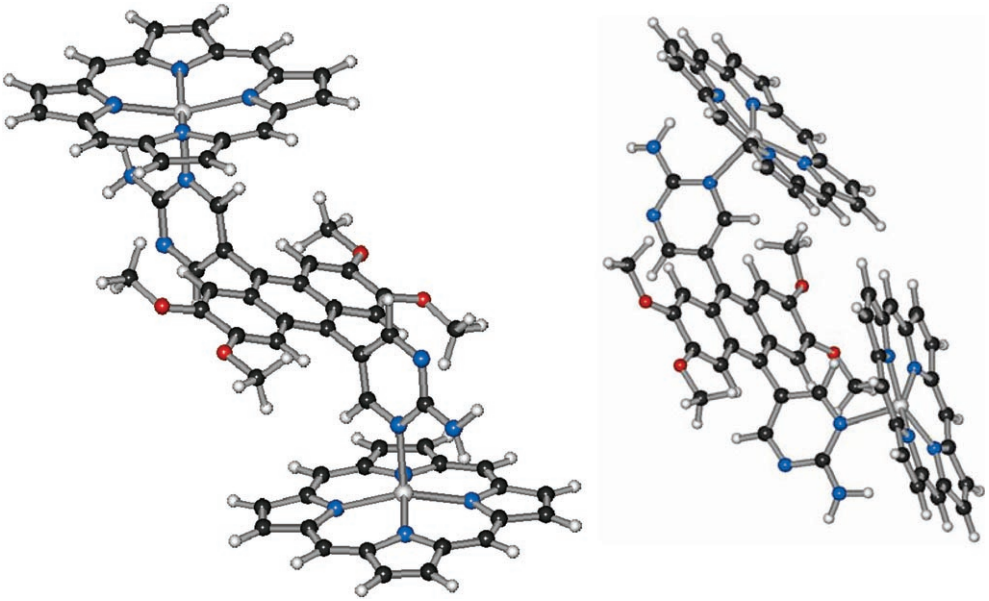

Fig. 7. *Probable molecular models for the rotamers of a complex* $\mathbf{7}\cdot\mathbf{19}_2$. Geometry optimization was performed within the HyperChem® package [20]. *meso*-Substituents of **19** were omitted from the calculation, while the crystal geometry of **7** was used in the optimizations.

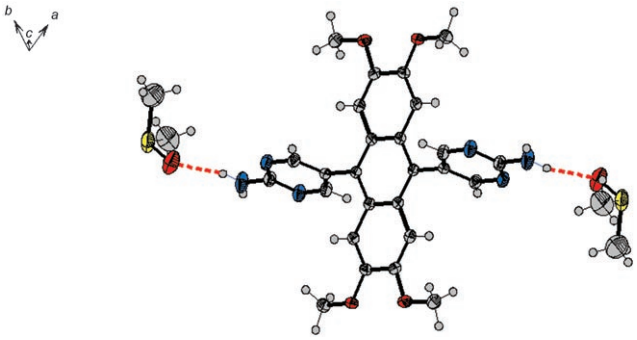

Fig. 8. *X-Ray structure of* **7**. Apparently, the S-atom (yellow) of the DMSO solvent molecules is slightly disordered as models fitted with a 9:1 distribution between two different position gives a significant improvement of the *R* factor. Only the major orientation is depicted. N- and O-Atoms are represented by blue and red ellipsoids, resp.

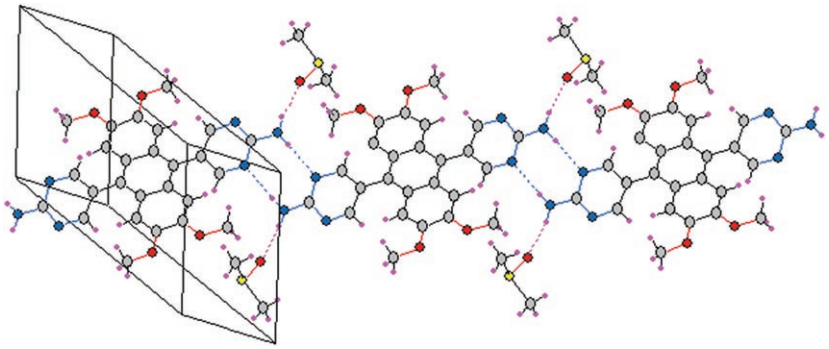

Fig. 9. *H-Bonding network in the crystal of* **7** *which leads to a planar tape.* S-Atoms are yellow, O-atoms red, N-atoms blue, and C-atoms gray, while protons are magenta.

The plane-to-plane spacing of *ca.* 3.45 Å in the crystal of **7** indicates quite tight π-stacking interactions. Interestingly, there exists an extensive overlap between the dimethoxy-substituted ends of the anthracene moieties. In the simple electrostatic model of the π–π interactions proposed by *Hunter* and *Sanders* [24] which predict off-setted geometries for extended π-systems such as porphyrins, an attractive interaction between the σ- and π-orbitals is balanced by the repulsion between the two π-sytems. In **7**, we note that two electron-rich regions are forced to overlap. Thus charge-transfer interactions do not operate. In principle the electron-rich regions of the anthracene moieties could have stacked with the electron-poor pyrimidine moieties. This, however would have resulted in less favorable H-bonding interactions between two adjacent pyrimidin-2-amines. Previously it has been observed that charge-transfer interactions are actually a particular case of π-stacking, which is the more general phenomenon. Thus, in phenyl-substituted pyrylium salts [25], this most electron-deficient 6-membered heteroarene ring π-stacks in the crystal with the much more electron-rich phenyl rings of adjacent molecules [26]. When the phenyl rings are electron poor, extended π-stacking is encountered, while with electron-rich phenyl rings, dimers are formed which

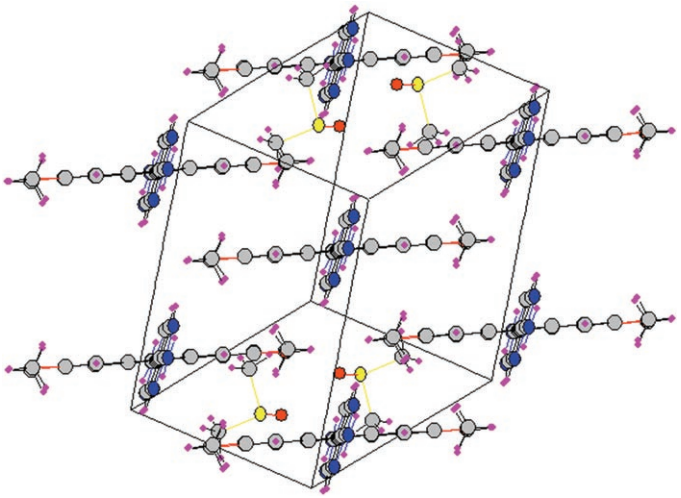

Fig. 10. *π-Stacking interactions in the crystal of* **7**

also give more deeply colored crystals due to partial charge transfer from the phenyl to the pyrylium ring [26]. It is also well known from dynamic NMR studies that the π–π interaction between electron-deficient aromatics is stronger than the one between an electron-poor and an electron-rich system, or the one between two electron-rich aromatic systems [27].

Conclusions. – Clearly a hierarchic self-assembly algorithm, beside dense crystal packing, operates in the case of **7**, with H-bonding, including also the crystallization solvent, being the dominant interaction. π-Stacking is the recessive interaction, and hydrophobic or dispersive forces which may act between the Me groups are probably negligible. The conformation of the MeO groups allows for close packing. If longer alkyl chains are present at the ether O-atoms, as in the case of **6**, probably dispersive forces may become dominant, and their interdigitation would lead to a completely different and more complicated crystal packing as shown for the 2,3-bis(hexyloxy)anthracene gelators [10]. We have reproducibly obtained nano- to microcrystals of **6** which tend to aggregate in fractal fashion but we have never observed gelating tendencies in our solutions. This lends support for the hypothesis that for anthracene gelators, in the absence of H-bonding groups, a dipole moment which packs the molecules (or higher assembly of polarized molecules) in a head to tail fashion is essential.

That the π–π interactions do operate in the crystal of **7** is an indication that the electron-rich anthracene rings cannot overlap in solutions of **6** as seen from absorption, fluorescence, and NMR studies. H-Bonding probably does occur between molecules of **6** in nonpolar solvents such as dry benzene or even dry $CHCl_3$ but these lead to assemblies without stacking. Thus, the 2PA recognition group is useful for solution self-assemblies only in the case when metal-ion ligation can operate, as was the case with the 2PA-substituted porphyrinatozincs **1** and **4**. Presently, it is not easy to estimate

the association constants for multiple supramolecular interactions which act in conjunction as either positive or negative cooperativity can be encountered.

Our study shows that predicting crystal packing(s) or polymorph formation with concomitant supramolecular interactions, in spite of continuing progress [28][29], is still a field with much room for improvement towards the goal of crystal engineering [30].

We are grateful to Professor *Jean-Pierre Vigneron* (Paris) for generously supplying us with a sample of 2,3,5,6-tetramethylphenazine which was used in the co-crystallization experiments, absorption studies, and ^{1}H-NMR titrations. *S. T. B.* was supported at ISIS (Strasbourg), where the main part of the experimental work was performed, by the Collège de France through a 'maître de conférences' position.

Experimental Part

General. $CHCl_3$ and $CDCl_3$ were dried by boiling overnight over P_2O_5 and were freshly distilled before spectroscopic measurements. C_6D_6 was dried by distillation from Na–K alloy. TLC: silica gel plates from *Macherey-Nagel*; elution with CH_2Cl_2 stabilized with 0.2% EtOH. Column chromatography (CC): *Merck* silica gel (40–63 μm). M.p.: *Büchi B-540* apparatus; in open capillaries; not corrected. UV/VIS Spectra: *Varian Cary-3* and *Cary-500* spectrometer, equipped with a *Peltier* variable-temp. unit; λ_{max} in nm (log ε_{max}). FT-IR Spectra: *Perkin-Elmer 1600* or *Spectrum GX* spectrometers; in cm^{-1}. NMR Spectra: *Bruker AC-200* spectrometer, at 200 (^{1}H) and 50.33 MHz (^{13}C); *Bruker DPX-300* spectrometer, at 300 MHz (^{1}H); chemical shifts δ in ppm rel. to residual nondeuterated solvent signal (for $CHCl_3$, δ 7.26 (^{1}H) and 77.0 (^{13}C); for (D_5)DMSO, δ 2.50 (^{1}H)), *J* in Hz. FAB-MS: by the Service de Spectrométrie de Mass de l'Université Louis Pasteur in Strasbourg; *Micromass-Autospec* instrument; 2-nitrobenzyl alcohol matrix; in *m*/*z* (rel. %). Elemental analyses; obtained either at the Service de Microanalyse de l'Université Louis Pasteur, Strasbourg, or at the Institute for Nanotechnology, Karlsruhe; *Carlo-Erba CEA* flash microanalyzer.

2,3,6,7-Tetrahydroxyanthracene-9,10-dione (**11**). A modification of the procedure reported by *Boldt* [9] was employed: 2,3,6,7-Tetramethoxyanthracene-9,10-dione (**10**; 7.51 g, 22.9 mmol) and 48% HBr soln. were heated under reflux (oil bath temp. 150°) for 3 days. After the first 24 h, more 48% HBr soln. (15 ml) was added through the reflux condenser to wash down some unreacted starting material which had collected there due to intense foaming and to its poor wettability. After 48 h, the yellow color had turned completely to ochre, and the foaming had stopped. After cooling, the precipitate was collected by filtration, washed to neutral pH with dist. H_2O, and air-dried: 6.36 g of crude **11** (102%). Purification was be accomplished after the next step. IR (KBr): 3406*s*, 1655*m*, 1580*s*, 1511*m*, 1321*s*, 1232*m*, 1160*m*, 1070*m*, 778*m*, 749*m*, 598*m*. ^{1}H-NMR ((D_6)DMSO; oven dried (110°) sample): 10.39 (sharp *s*, OH; br. signal in wet samples); 7.43 (*s*, arom. H); 3.94 (residual *s*, MeO of some contaminating unhydrolyzed product).

2,3,6,7-Tetrakis(decyloxy)anthracene-9,10-dione (**12**). The crude **11** (5.0 g, 18.3 mmol) was finely ground in a mortar and then transferred to a reaction flask. DMF (100 ml) and anh. K_2CO_3 (17.64 g) were added to the flask after rinsing the mortar. Then 1-bromodecane (40.34 g, 183 mmol) was added, and the mixture was stirred for 5 min under Ar bubbling for degassing after which the flask was stoppered with an Ar-filled balloon. Stirring was continued at r.t. for 90 min, and then the mixture was heated gently to 60°. After 1/2 h at 60°, the mixture gelified completely, and an efficient magnetic stirrer was needed to stir the mixture overnight at this temp. Then, dist. H_2O (80 ml) was added to dissolve the excess K_2CO_3 and to break up the cake. The mixture was cooled in an ice-water bath and then filtered. The kaki-colored precipitate was washed with dist. H_2O (3×), 50% aq. MeOH (1×), and lastly with cold MeOH. Isolation of additional product from the dark-colored filtrate by CC proved uneconomical, so the filtrate was discarded. The crude product was recrystallized from boiling toluene (250 ml): 10.65 g (69.6% yield) of pure **12**, free of the MeO-substituted contaminant. R_f (CH_2Cl_2) 0.76. M.p. 139–140°. UV (CH_2Cl_2): 280 (sh., 4.84), 293 (5.11), 345 (4.40). IR (KBr): 2918*s*, 2850*s*, 1662*m*, 1575*s*, 1512*m*, 1466*m*, 1368*m*, 1329*s*,

1227*m*, 1077*m*, 1063*m*, 892*w*, 742*m*, 616*w*. ^{1}H-NMR (200 MHz, $CDCl_3$): 7.64 (*s*, H–C(1), H–C(4), H–C(5), H–C(8)); 4.18 (*t*, *J* = 6.5, 4 CH_2O), 1.89 (*quint*., 8 H); 1.28 (sharp *m*, 56 H); 0.88 (*t*, 4 Me). FAB-MS: 833.8 (100, $[M+H]^+$), 693.6 (51, $[M+H-C_{10}H_{20}]$), 553.5 (20, $[M+H-2\,C_{10}H_{20}$). Anal. calc. for $C_{54}H_{88}O_6$: C 77.84, H 10.64; found: C 77.51, H 10.51.

*2,3,6,7-Tetrakis(decyloxy)anthracen-9(10*H*)-one* (**13**). Zn-Powder (16.9 g) was activated by stirring for 10 min with a soln. of $CuSO_4$ (0.4 g) in H_2O (250 ml). The aq. soln. was decanted, and 10% NaOH soln. (160 ml), **12** (8.67 g, 10,4 mmol), and toluene (150 ml) were added to the Zn-powder. The mixture was heated overnight on an oil bath at 120° maintaining vigorous boiling and magnetic stirring (the aq. layer became reddish while the yellow toluene layer discolored slowly as the reaction proceeded). Then, the toluene layer was decanted while still warm from the orange-red aq. layer and washed once with warm H_2O and separated by decantation from all the unreacted Zn-powder. Refrigeration and seeding produced crystals which were filtered off and dried: 7.35 g (86%) of crude **13**, contaminated by a small amount of the anthracene (TLC, NMR). Longer reaction times did not increase the yield in anthracene. Extraction with CH_2Cl_2 of the aq. layer and combining it with the toluene filtrate yielded an additional 1.31 g of material which was subjected to CC (silica gel, CH_2Cl_2). TLC (CH_2Cl_2): R_f 0.68; spots became yellow by and by probably due to back conversion to the anthracenedione. UV (CH_2Cl_2): 284, 337. IR (KBr): 2918*s*, 2848*s*, 1648*w*, 1596*s*, 1513*s*, 1467*m*, 1382*m*, 1334*s*, 1262*s*, 1228*s*, 1091*s*. ^{1}H-NMR (200 MHz, $CDCl_3$): 7.79 (*s*, H–C(1), H–C(8)); 6.82 (*s*, H–C(4), H–C(5)); 4.13 (*s*, CH_2(10)); 4.08 (*t*, *J* = 6.6, 4 CH_2O); 1.87 (br. *quint*., 8 H); 1.48 (br. *m*, 8 H); 1.28 (sharp *m*, 48 H); 0.88 (*t*, 4 Me). ^{13}C-NMR (50 MHz, $CDCl_3$): 182.5 (CO); 153.1; 148.40; 135.0; 125.4; 111.1; 110.3; 69.2 (OCH_2); 32.0; 29.7; 29.5; 29.24; 29.17; 26.1; 22.8; 14.2. FAB-MS: 819.9 (100, $[M+H]^+$), 791.8 (13, $[M+H-CO]^+$), 679.7 (23, $[M+H-C_{10}H_{20}]^+$).

2,3,6,7-Tetrakis(decyloxy)anthracene (**14**). By warming gently, **13** (7.35 g, 8.98 mmol) was dissolved in CH_2Cl_2 (200 ml). Ar was then bubbled through the soln. for 5 min. Powdered $NaBH_4$ (5.25 g, 135 mmol) was added, and then MeOH (30 ml) was added dropwise under stirring at r.t. After the addition was completed, foaming started. After 90 min, when the foaming subsided, a fresh portion of $NaBH_4$ (1.5 g) was added. The reaction was quenched after 7 h by adding carefully and dropwise AcOH (10 ml). Extensive foaming could be controlled by adding small portions of CH_2Cl_2. The mixture was then left to stand overnight. Then AcOH (5 ml) was added until no more foaming occurred, and then carefully conc. HCl soln. (10 ml). At the end of the addition, the mixture became slightly greenish. Stirring was continued for 5 min after which H_2O (50 ml) was added. The CH_2Cl_2 layer, which contained a fine precipitate, was washed with H_2O (200 ml) and then filtered. The colorless precipitate was washed repeatedly with H_2O until the filtrate had neutral pH and dried: 5.4 g (75%) of **14**, pure by TLC and NMR. Interestingly, this long-chain-substituted anthracene is completely unwettable. Additional 0.24 g of **14** could be obtained from the filtrate: Thus, the yellowish CH_2Cl_2 filtrate was washed once with H_2O, then with aq. $NaHCO_3$ soln., then again with H_2O, dried (Na_2SO_4), concentrated, and deposited onto silica gel. CC (hexane/CH_2Cl_2 1:1) separated neatly **14** from some corresponding 9,10-dihydroanthracene (180 mg) and unreacted **13**. An anal. sample of **14** was obtained by recrystallization from toluene.

TLC (CH_2Cl_2/hexane 1:1): R_f 0.63 (**14**); 0.47 (dihydro derivative), 0.18 (**13**). **14**: M.p. 160–161°. UV (CH_2Cl_2): 271 (5.23), 372 (4.30). IR (KBr): 2956*m*, 2918*s*, 2852*s*, 1492*s*, 1467*s*, 1241*s*, 1167*m*, 893*m*. ^{1}H-NMR (200 MHz, $CDCl_3$): 7.95 (*s*, H–C(9), H–C(10)); 7.11 (*s*, H–C(1), H–C(4), H–C(5), H–C(8)); 4.12 (*t*, *J* = 6.6, 4 CH_2O); 1.91 (br. *quint*., 8 H); 1.50 (br. *m*, 8 H); 1.28 (sharp *m*, 48 H); 0.88 (*t*, 4 Me). EI-MS: 802.9 (100, M^+), 662.6 (8, $[M-C_{10}H_{20}]^+$), 241.7 (20). FAB-MS (a variety of matrices): no signals. Anal. calc. for $C_{54}H_{90}O_4$: C 80.74, H 11.29; found: C 80.50, H 11.03.

9,10-Dibromo-2,3,6,7-tetrakis(decyloxy)anthracene (**15**). Compound **14** (2.41 g, 3.0 mmol) was dissolved in boiling CCl_4 (100 ml) and filtered while hot. After cooling to r.t., Br_2 (1.20 g, 0.38 ml, 7.5 mmol) was added *via* syringe. The mixture was heated (100° bath temp.) to a gentle boil when HBr started to evolve. The reaction was stopped after 35 min at reflux, the mixture cooled, and the precipitate filtered and dried: 1.10 g of **15**. An additional crop (0.885 g) was obtained by evaporating the filtrate and recrystallizing the residue from boiling CCl_4 (15 ml), increasing thus the yield to 69%. R_f(CH_2Cl_2/hexane 1:1) 0.77. UV (CH_2Cl_2): 282, 384. IR (KBr): 2954*m*, 2921*s*, 2850*s*, 1505*s*, 1496*s*, 1464*s*, 1251*s*, 1167*s*, 831*m*. ^{1}H-NMR (200 MHz, $CDCl_3$): 7.67 (*s*, H–C(1), H–C(4), H–C(5), H–C(8)); 4.21 (*t*, *J* = 6.6, 4 CH_2O); 1.96

(*quint.*, 8 H); 1.50 (br. *m*, 8 H); 1.28 (sharp *m*, 48 H); 0.89 (t, 4 Me). ^{13}C-NMR (50 MHz, $CDCl_3$): 150.6; 126.5; 106.5; 101.6; 68.91; 29.6; 29.44; 29.37; 29.0; 26.1; 22.7; 14.1. EI-MS: 961.5 (100, M^+, isotopic pattern), 933.4 (50, isotopic pattern), 400.1 (60).

5,5′-[2,3,6,7-Tetrakis(decyloxy)anthracene-9,10-diyl]bis[pyrimidin-2-amine] (**6**). An oven-dried flask was charged with **15** (1.092 g, 1.136 mmol), 2-[5-(trimethylstannyl)pyrimidin-2-yl]-1*H*-isoindol-1,3(2*H*)-dione [3] (**16**; 1.102 g, 2.842 mmol), and toluene (25 ml) freshly distilled from Na dispersion. Ar was bubbled through the mixture for 5 min after which tetrakis(triphenylphosphine)palladium catalyst (65.6 mg, 0.056 mmol) was added. Ar bubbling was continued for 2 min after which the flask was stoppered with an Ar-filled balloon. The mixture was heated to $100\pm5°$ as it became homogeneous, translucent pale yellow. Heating was continued for 22 h. Cooling to $-18°$ produced a fine precipitate which was filtered with difficulty and washed with two portions of CH_2Cl_2. Deprotection was performed by suspending this precipitate in CH_2Cl_2 (400 ml) and treatment with methylhydrazine (8 ml). The mixture which became blueish fluorescent contained a fine precipitate which was stirred for 2 h at r.t. Silica gel (8 g) was added and the mixture evaporated (*Caution:* the dry silica gel with excess methylhydrazine, after removing from the rotary evaporator, may overheat so that careful handling (insulating gloves) and cooling is recommended). CC (silica gel, 10% EtOH/$CHCl_3$) produced a yellow band which yielded 1.021g (90.9% over two steps) of pure **6**. An anal. sample was recrystallized from 1,2-dichloroethane. R_f (EtOH/$CHCl_3$ 2:10) 0.82. M.p. 248° (yellow melt). UV ($CHCl_3$): 276, 383 (see also *Fig. 11*). IR (KBr): 3340*m*, 3186*m*, 2924*s*, 2853*ms*, 1659*s*, 1595*ms*, 1496*vs*, 1465*s*, 1351*m*, 1244*s*, 1208*m*, 1142*m*, 841*m*, 806*m*. ^{1}H-NMR (200 MHz, $CDCl_3$): 8.41 (*s*, 4 H, H–C(4), H–C(6) (py)); 6.81 (*s*, H–C(1), H–C(4), H–C(5), H–C(8) (anth)); 5.24 (*s*, D_2O exchange, 2 NH_2); 3.91 (*t*, $J=6.4$, 4 CH_2O); 1.81 (*quint.*, 8 H); 1.43 (br. *m*, 8 H); 1.27 (sharp *m*, 48 H); 0.88 (*t*, 4 Me). ^{13}C-NMR (50 MHz, $CDCl_3$, 50°): 162.4; 160.2; 149.9; 127.0; 123.5; 105.3; 69.1 (CH_2O); 31.9; 29.62; 29.55; 29.43; 29.32; 29.1; 26.1; 22.6; 14.0 (Me); the seventh arom. C (probably C(2) of pyrimidine) resonated at δ *ca.* 126 (br., due to the proximity of the 3 N-atoms). FAB-MS: 989.8 (100, $[M+H]^+$), 848.6 (16, $[M-C_{10}H_{20}]^+$). Anal. calc. for $C_{62}H_{96}N_6O_4$: C 75.26, H 9.78, N 8.49; found: C 75.24, H 9.59, N 8.19.

Complex of **6** *with TCNE*. Ethenetetracarbonitrile (TCNE) was added to a warm $CHCl_3$ soln. of **6** when a blue precipitate formed rapidly which could be filtered with difficulty under Ar. The starting **6** was recovered unchanged after addition of acetone which bleached the blue powder. Blue powder: M.p. >400° (dec.). ^{1}H-NMR: no differences from the spectrum of uncomplexed **6**. ^{13}C-NMR (50 MHz,

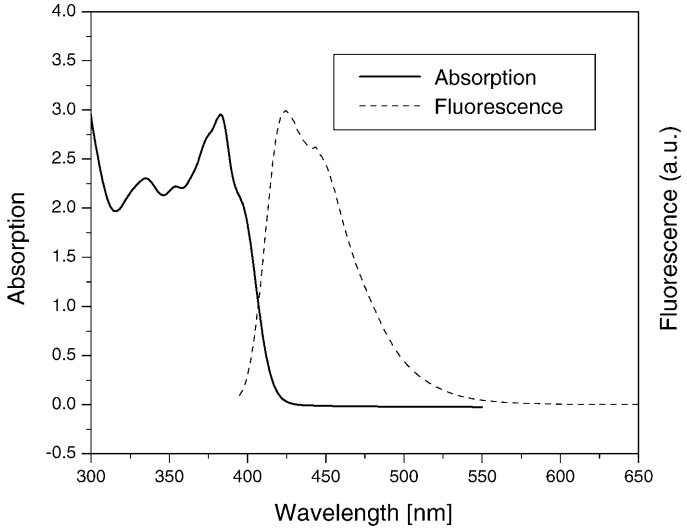

Fig. 11. *Absorption and fluorescence spectra of* **6** *in* CH_2Cl_2 (excitation wavelength 380 nm)

$CDCl_3$, 50°): 160.2; 149.8; 127.0; 123.5; 105.1; 69.0; 31.94; 29.64; 29.57; 29.44; 29.34; 29.1; 26.2; 22.7; 14.0; only 5 arom. C were visible, the δ(C) 162.4 of **6** was absent, and no TCNE C-signal was detected. Anal. calc. for $C_{68}H_{96}N_{10}O_4$ (**6**·TCNE): C 73.08, H 8.66, N 12.53; found: C 70.89, H 8.64, N 12.40.

9,10-Dibromo-2,3,6,7-tetramethoxyanthracene (**18**). Bromination of 2,3,7,8-tetramethoxyanthracene (**17**) [14] which was recrystallized from hot nitrobenzene on a gram scale, was performed as described for **15**, except that the suspension of **17** in CCl_4 was not filtered. The product was purified by boiling with toluene and triturating and was used in the next step. UV ($CDCl_3$): 278, 380 (rel. extinct. 7.8 : 1). ^{1}H-NMR (200 MHz, $CDCl_3$): 7.68 (*s*, H–C(1), H–C(4), H–C(5), H–C(8)); 4.11 (*s*, 4 MeO). ^{1}H-NMR (200 MHz, (D_6)DMSO): 7.65 (*s*, H–C(1), H–C(4), H–C(5), H–C(8)); 4.01 (*s*, 4 MeO). ^{13}C-NMR (50 MHz, $CDCl_3$, 50°): 150.7; 126.6; 105.6 (CH); 56.0 (MeO); due to the low solubility, the quaternary C was not visible after an overnight accumulation. FAB-MS: 456.0 (100, $[M+H]^+$), 442.0 (50, $[M-Me]^+$), 426 (38, $[M-2\,Me]^+$), 413.2 (38); abundant ions below *m*/*z* 350 due to extensive fragmentation of the anthracene skeleton; the low signal to noise ratio indicates the high stability of the parent ion.

5,5′-(2,3,6,7-Tetramethoxyanthracene-9,10-diyl)bis[pyrimidin-2-amine] (**7**). *Stille* coupling of the stannyl derivative **16** (669 mg, 250 mol-%) with **17** (315 mg) and tetrakis(triphenylphosphine)palladium catalyst (40 mg, 5 mol-%) was performed in dry toluene (20 ml) by heating at 100° for 56 h. Due to the low solubility of **17**, the mixture was heterogeneous, and the reaction could not be driven to completion. After deprotection with methylhydrazine similarly as described for **6**, CC (silica gel, 10% EtOH/$CHCl_3$) yielded several fractions. After impure fractions (100 mg) containing also starting material, the monocoupled product was eluted which was recrystallized from $CHCl_3$/EtOH 98 : 2. After mixed fractions, pure **7** (250 mg) was obtained. No optimization of the reaction was attempted. Single crystals of **7** were grown from DMSO upon dissolution under gently heating, cooling to r.t., and slow evaporation over 12 months. Co-crystallization experiments with phenazine or 1,4,5,8-tetramethylphenazine from either hot DMSO or MeCN/DMSO did not yield inclusion complexes but the same crystalline hexagonal plates of **7** were obtained. In some trials, yellow needles of phenazine even crystallized preferentially instead.

Data of **7**: M.p. > 400° (dec.). ^{1}H-NMR (200 MHz, (D_6)DMSO): 8.32 (*s*, 4 H, H–C(4), H–C(6) (py)); 6.86 (br.), 6.84 (2*s*, 2 NH_2, H–C(1), H–C(4), H–C(5), H–C(8) (anth)); 3.71 (*s*, 6 CH_2O); solvent (2.50), H_2O (3.30), and a broad peak at δ *ca.* 1 were also visible. FAB-MS: 484.3 ($C_{26}H_{24}N_6O_4^+$,$[M+H]^+$; calc. 484.19); no other peaks over 35%.

Monocoupled Product 5-(10-Bromo-2,3,6,7-tetramethoxyanthracen-9-yl)pyrimidin-2-amine[6]) ^{1}H-NMR (200 MHz, (D_6)DMSO): 8.38 (*s*, H–C(4), H–C(6) (py)); 7.75 (*s*, H–C(1), H–C(8) (anth)); 6.78 (*s*, H–C(4), H–C(5) (anth)); 5.23 (br. *s*, 2 H); 4.11 (s, MeO–C(2), MeO–C(7)); 3.84 (*s*, MeO–C(3), MeO–C(6)); solvent (7.26), H_2O (1.550), and a broad peak at δ *ca.* 1.6 were also visible. FAB-MS: 469, 471.2 (isotopic pattern, $C_{22}H_{21}{}^{79}BrN_3O_4^+$, $[M+H]^+$; calc. 470.1); no other peaks over 6%.

Crystallographic Data of **7**. The data collections were carried out on a *Stoe-IPDS-I* diffractometer equipped with a *Schneider* rotating anode by using graphite-monochromated Mo-$K\alpha$ (λ 0.71073 Å) radiation at 200 K. The structure solutions and full matrix least-square refinements based on F^2 were performed with the SHELX-97 program package [31]. Molecular diagrams were prepared with the program Diamond [32]. Data for **7**[7]): Rhombic plates, 0.22×0.2×0.05 mm, M_r 784.5, triclinic, space group $P\bar{1}$ (No. 2), a=8.206(2), b=8.633(2), c=12.681(3) Å, α=71.26(3), β=85.91(3), γ=67.47(3)°, V=784.5(3) Å^3, Z=1, D_c=1.356 g cm^{-3}, μ(Mo-$K\alpha$)=0.222 mm^{-1}. All O-, N-, C-, and S-atoms were refined with anisotropic displacement parameters with a 10% disorder of the S-atom. H-Atoms were added in calculated positions to give a final R_1 value of 0.0617 for 208 parameters and 2479 unique reflections with $I \geq 2\sigma(I)$ and wR_2 of 0.1804 for all 7012 reflections (R_{int}=0.1409).

---

[6]) This by-product may be useful in a second Pd-catalyzed aryl–aryl coupling with a different recognition group, or with the same pyrimidin-2-amine but protected otherwise than with phthalimide to assure orthogonality.

[7]) CCDC-285563 contains the supplementary crystallographic data for this paper. These data can be obtained free of charge from the *Cambridge Crystallographic Data Centre via* www.ccdc.cam.ac.uk/data_request/cif.

REFERENCES

[1] M. J. Krische, J.-M. Lehn, N. Kyritsakas, J. Fischer, *Helv. Chim. Acta* **1998**, *81*, 1909.
[2] M. J. Krische, J.-M. Lehn, N. Kyritsakas, J. Fischer, E. K. Wegelius, M. J. Nissinen, K. Rissanen, *Helv. Chim. Acta* **1998**, *81*, 1921.
[3] M. J. Krische, J.-M. Lehn, N. Kyritsakas, J. Fischer, E. K. Wegelius, K. Rissanen, *Tetrahedron* **2000**, *56*, 6701.
[4] T. S. Balaban, R. Goddard, M. Linke-Schaetzel, J.-M. Lehn, *J. Am. Chem. Soc.* **2003**, *125*, 4233.
[5] A. Tsuda, S. Sakamoto, K. Yamaguchi, T. Aida, *J. Am. Chem. Soc.* **2003**, *125*, 15722.
[6] M. Vinodu, Z. Stein, I. Goldberg, *Inorg. Chem.* **2004**, *43*, 7582.
[7] M. J. Crossley, P. L. Burn, *J. Chem. Soc., Chem. Commun.* **1987**, 39.
[8] A. Müller, M. Raltschewa, M. Papp, *Chem. Ber.* **1942**, *75*, 692.
[9] P. Boldt, *Chem. Ber.* **1967**, *100*, 1270.
[10] T. Brotin, R. Utermöhlen, F. Fages, H. Bouas-Laurent, J.-P. Desvergne, *J. Chem. Soc., Chem. Commun.* **1991**, 416.
[11] J.-L. Pozzo, J.-P. Desvergne, G. M. Clavier, H. Bouas-Laurent, P. G. Jones, J. Perlstein, *J. Chem. Soc., Perkin Trans. 2* **2001**, 824.
[12] A. Petitjean, R. G. Khoury, N. Kyritsakas, J.-M. Lehn, *J. Am. Chem. Soc.* **2004**, *126*, 6637.
[13] B. M. Trost, *Science* (*Washington, D.C.*) **1991**, *254*, 1471.
[14] P. W. Rabideau, *J. Org. Chem.* **1971**, *36*, 2723.
[15] J.-M. Lehn, F. Schmidt, J.-P. Vigneron, *J. Heterocycl. Chem.* **1990**, *27*, 1633.
[16] T. S. Balaban, A. Eichhöfer, J.-M. Lehn, *Eur. J. Org. Chem.* **2000**, 4047.
[17] S. Matile, N. Berova, K. Nakanishi, *J. Am. Chem. Soc.* **1995**, *117*, 7021.
[18] S. Matile, N. Berova, K. Nakanishi, J. Fleischhauer, R.W. Woody, *J. Am. Chem. Soc.* **1996**, *118*, 5198.
[19] P. Ballester, A. Costa, A. M. Castilla, P. M. Deyà, A. Frontera, R. M. Gomilla, C. A. Hunter, *Chem.–Eur. J.* **2005**, *11*, 2196.
[20] 'HyperChem®', Release 7 Professional Version, HyperCube Inc., Gainesville, Florida, 2002.
[21] J. M. Masnovi, J. K. Kochi, E. F. Hilinski, P. M. Rentzepis, *J. Phys. Chem.* **1985**, *89*, 5387.
[22] J. M. Masnovi, J. K. Kochi, E. F. Hilinski, P. M. Rentzepis, *J. Am. Chem. Soc.* **1986**, *108*, 1126.
[23] A.-F. Mourad, A. Akkermann-Kubillus, J. Hucker, *J. Prakt. Chem.* **1988**, *330*, 15.
[24] C. A. Hunter, J. K. M. Sanders, *J. Am. Chem. Soc.* **1990**, *112*, 5525.
[25] T. S. Balaban, A. T. Balaban, in 'Science of Synthesis, Vol. 14', E. J. Thomas, Thieme, Stuttgart, 2003, p. 11–200.
[26] T. S. Balaban, N. Furmanova, *Z. Naturforsch., B* **1997**, *52*, 485.
[27] F. Cozzi, J. S. Siegel, *Pure Appl. Chem.* **1995**, *67*, 683.
[28] A. Gavezzotti, *Acc. Chem. Res.* **1994**, *27*, 309.
[29] J. D. Dunitz, A. Gavezzotti, *Acc. Chem. Res.* **1999**, *32*, 677.
[30] G. Desiraju, 'Crystal Engineering: The Design of Organic Solids', Elsevier, New York, 1989.
[31] G. M. Sheldrick, 'SHELX-97, Program for X-Ray Crystal Structure Determination and Refinement', Göttingen University, Göttingen, 1997.
[32] 'Diamond, V. 3.0', Crystal Impact GbR, Bonn, 15. October, 2004.

Received October 19, 2005